Research in Astronomy and Astrophysics, 22:015014 (8pp), 2022 January https://doi.org/10.1088/1674-4527/ac3895

The Variability of the Narrow-line Seyfert 1 Galaxies from the Pan-STARRS's View

Hong-Tao Wang[1], Yan-Ping Su[2], Xue Ge[3], Yong-Yun Chen[4], and Xiao-Ling Yu[5]
[1] School of Science, Langfang Normal University, Langfang, 065000, China; wanghongtao@lfnu.edu.cn
[2] School of Life Science, Langfang Normal University, Langfang, 065000, China
[3] School of Physics and Electronic Engineering, Jiangsu Second Normal University, Nanjing, Jiangsu 211200, China
[4] The College of Physics and Electronic Engineering, Qujing Normal University, Qujing, 655011, China
[5] School of Astronomy and Space Science, Nanjing University, Nanjing, 210093, China
Received 2021 April 13; revised 2021 September 27; accepted 2021 September 28; published 2022 January 21

Abstract

By means of the data sets from the Pan-STARRS1 survey, we have systematically examined the relationship between the variability characteristics and the physical parameters of the largest NLS1 galaxy sample up to now. The results are summarized as follows: (1). We find significant anti-correlations between variability amplitude and absolute magnitude in g, r, i, z and y bands, which are consistent with the results in previous works. (2) The correlations between the variability amplitude in optical band and many physical parameters (e.g., λL(5100 Å), black hole mass, Eddington ratio, R_{4570} and R_{5007}) are investigated. The results show the variability amplitude is significantly anti-correlated with L(5100 Å), $M_{\rm BH}$, Eddington ratio and R_{4570}, but positively correlated with R_{5007}. The relation could be explained by the simple standard accretion disk model. (3) We further investigate the relationship between optical variability and radio luminosity/radio-loudness. The results present weak positive correlation in g and r bands, but insignificant correlation in i, z and y bands. The large error of the approximate fraction of the host galaxy in i, z and y bands may lead to insignificant correlations.

Key words: catalogs – galaxies: photometry – galaxies: Seyfert

1. Introduction

The optical variability of active galactic nuclei (AGNs) has been found since their discovery (Matthews & Sandage 1963). Irregular variability of quasars/AGNs is ubiquitous across all wave bands (Ulrich et al. 1997). It is generally recognized that the emission in optical band originates from the thermal radiation in the accretion disk surrounding supermassive black holes (SMBHs). The typical variability amplitude usually shows less than two magnitudes within the timescale of a few months to years (e.g., Ivezic et al. 2004; Vanden Berk et al. 2004). The optical variability carries much valuable information, which could be used to trace the physical processes around SMBHs (Guo et al. 2017).

Optical variation on the order of hours to years is one of the main features of AGNs. The optical variability of quasars/AGNs is irregular and complicated. It is commonly believed that the emission in optical band originates from optically thick accretion disk driven by the central SMBH, but the physical processes producing its variability are not clearly understood. However, the statistical study of the variability sample on fundamental physical parameters provides a new view for us to uncover the variability mechanisms. Many investigations of AGN/quasars indicated that the variability was correlated with wavelength (e.g., di Clemente et al. 1996; Helfand et al. 2001), luminosity (e.g., Hawkins 2000; Lu et al. 2019), time lag (e.g., de Vries et al. 2005) and redshift (e.g., Vanden Berk et al. 2004; Meusinger et al. 2011; Welsh et al. 2011). Some results showed the variability was correlated with $M_{\rm BH}$ (e.g., Bauer et al. 2009; Zuo et al. 2012; Lu et al. 2019), and anti-correlated with the Eddington ratio (e.g., Ai et al. 2010; MacLeod et al. 2010; Lu et al. 2019).

Seyfert galaxies are a subclass of AGNs, which are generally classified into Seyfert 1 and Seyfert 2 galaxies. Seyfert 1 galaxies usually present the broad emission line of a few thousand km s^{-1} originating from the broad line region (BLR). Seyfert II galaxies show emission line less than 1000 km s^{-1} from the narrow line region (NLR). Narrow-line Seyfert 1 (NLS1) galaxies have a narrow Hβ line with the full width at half maximum (FWHM) < 2000 km s^{-1} and weak [O III] emission line with the flux ratio F([O III])/F(Hβ) < 3 (Osterbrock & Pogge 1985). Some results show that NLS1 galaxies have smaller black hole mass $\sim 10^7$ $M_\odot$ and higher accretion rate (Xu et al. 2012). However, other results indicate a smaller black hole mass may arise from the effect of the inclination angle of BLR (Decarli et al. 2008).

A few variability studies on NLS1 galaxies were investigated previously. Only a few objects have much longer light curves, e.g., the optical variability (e.g., Doroshenko et al. 2006; Shapovalova et al. 2012) and the X-ray variability of Ark 564

Table 1
Basic Parameter Information on Pan-STARRS, CRTS, PTF/iPTF, ZTF and SDSS Stripe 82

	Observation Band	5σ Depth/mag	Time Baseline	Cadence
SDSS Stripe 82	u, g, r, i, z	23.9, 25.1, 24.6, 24.1, 22.8	1998–2007	∼1 epoch/month
CRTS/CSS,MLS	V	∼20	2003–2016	$1\sim4$ times/month
CRTS/SSS	V	∼19	2005–2013	$1\sim4$ times/month
PTF	R, g	R(20.5), g(21.0)	2009–2012	a 5 day cadence
iPTF	R, g	R(20.5), g(21.0)	2013–2017	a 5 day cadence
ZTF	g, r, i	g(21.0), r(20.4),i(20.5)	Nov,2017- now	a 3 day cadence
Pan-STARRS	g, r, i, z, y	23.3, 23.2, 23.1, 22.3, 21.3	2010–2014	∼12 epochs/month

(Gliozzi et al. 2002), and the variability of 113 bright soft X-ray AGNs (Grupe et al. 2001). The above results show the NLS1 galaxies usually have low variability. Based on the optical variability of six NLS1 galaxies, Klimek et al. (2004) found that NLS1 galaxies were less variable than broad-line Seyfert 1 (BLS1) galaxies on long timescales in optical band, which could be explained by the negative correlation between variability amplitude and Eddington ratio, if NLS1 galaxies actually had high accretion rate. Ai et al. (2010) analyzed the variability amplitude (σ_d) of 58 NLS1 and 217 BLS1 galaxies by the multi-epoch photometric data sets in Stripe 82 from Sloan Digital Sky Survey (SDSS). The results showed significant and robust negative correlation between σ_d and $\lambda_{\rm Edd}$. Ai et al. (2013) further investigated the variability by an ensemble method. In their results, the majority of NLS1 galaxies presented significant variability on a timescale larger than 10 days, but smaller variability amplitude compared to BLS1 galaxies. In a timescale of less than 10 days, NLS1 galaxies may have different variability mechanisms compared with BLS1 galaxies, such as X-ray reprocessing which may appear in BLS1 AGNs, however, this does not occur in NLS1 AGNs. Compared with their broad line counterparts, the long-term optical variability of NLS1 galaxies had been investigated by Rakshit & Stalin (2017), in which a large number of objects were analyzed by the catalog of Rakshit et al. (2017) with optical data from the Catalina Real-Time Transient Survey (CRTS). They found that NLS1 galaxies as a class feature lower variability amplitude than their broad-line counterparts. In addition to the long-term optical variability, the characteristics of intra-night optical variability in different categories of NLS1 galaxies are also well studied (Maune et al. 2013; Paliya et al. 2013; Kshama et al. 2017). In summary, the statistical regularity of optical variability in NLS1 galaxies is relatively scarce and should be further investigated.

The Panoramic Survey Telescope and Rapid Response System (Pan-STARRS, see more details in Section 2) was operating in 2014. The photometric uncertainties of Pan-STARRS is lower than that in PTF/iPTF, ZTF and CRTS. The other basic parameters are listed in Table 1, which show much deeper observation than those in PTF/iPTF, ZTF and CRTS. The cadence is higher than those in SDSS, PTF/iPTF, ZTF and CRTS. Comparing with CRTS in Rakshit & Stalin (2017), there are five photometric bands with much smaller error from Pan-STARRS, and the 5 sigma limiting magnitude ∼21–23 mag of Pan-STARRS is much deeper than 19 mag in CRTS. The cadence of ∼12 epochs of Pan-STARRS is much higher than $1\sim4$ epochs of CRTS. The sample provided by Rakshit et al. (2017) is the largest one, which contains 11 101 NLS1 galaxies and was suitable for us to investigate the variability characteristics. Pan-STARRS, with data sets featuring small photometric error, high cadence and long time baseline, gives us a new chance to further investigate the variability characteristics of NLS1 galaxies.

The paper is organized as follows. We describe the data sets and sample selection in Section 2. In Section 3, we introduce the analytical method. The results and discussions are presented in Section 4. The conclusions are given in Section 5.

2. Data

In this work, we have taken the 11 101 NLS1 galaxies sample from the catalog of Rakshit et al. (2017), which was based on the spectroscopic database of the SDSS Data Release 12 (DR12; Alam et al. 2015).

The optical data sets are from Pan-STARRS which is operated by the Institute for Astronomy at the University of Hawaii. The facility has a wide-field astronomical imaging system. Pan-STARRS1 (PS1) is the result in the first stage of Pan-STARRS. It was completed and the database was released in Data Release 1 and 2 (DR1 and DR2). A 1.8 m telescope with a 1.4 gigapixel camera was used to image the sky in five broadband filters (g, r, i, z and y) during the PS1 survey, which covers the region of the north of decl. −30 degree. The PS1 Science Mission started operation in March 2014, and the PS1 DR2 occurred on 2019 January 28. We cross match the NLS1 galaxy sample with the Pan-STARRS1 database by the matching radius of 3″, then obtain the light curve of 11 101 samples. The maximum, minimum and median values of the time baseline are 5.6 yr, 1 day and $3.0\sim3.7$ yr in these five bands, respectively. The maximum, minimum and median values of the number of epochs are 134, 2, and 12–20, respectively. Because the AGN variability

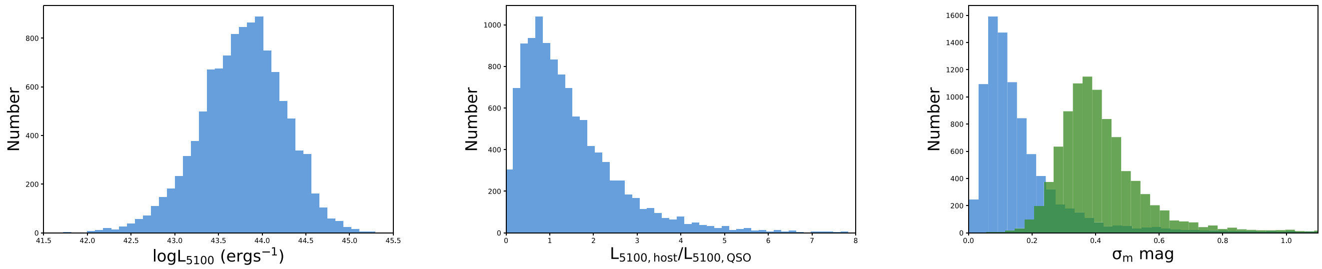

Figure 1. The distribution of luminosity at 5100 Å, the fractional host contamination at 5100 Å and the variability amplitude in *r* band (The green histogram is revised by the host galaxy contamination and the blue one is not revised.) for NLS1 galaxy sample, from left to right, respectively.

Table 2
The Data Information in the NLS1 Galaxy Sample

Band	Epoch Number Maximum	Epoch Number Minimum	Epoch Number Median Value	Time Baseline/Day Maximum	Time Baseline/Day Minimum	Time Baseline/Day Median Value
g	70	5	12	1607.7	730.1	1096.0
r	78	5	14	1899.8	730.0	1176.8
i	134	5	20	1925.7	730.1	1503.0
z	54	5	13	2070.4	730.0	1363.1
y	70	5	12	1970.6	730.9	1428.0

amplitude is strongly related to the observed time interval, we select a time baseline longer than two years, thus 8078, 8955, 9318, 8777 and 7343 objects are left in g, r, i, z and y bands, respectively. The mechanism of the radio-loud NLS1 galaxies in optical band originates from the relativistic jet, thus the impact of the radio-loud objects should be eliminated. When we cross match the sample with the Faint Images of the Radio Sky at Twenty-Centimeters (FIRST) survey, 555 objects are found. Considering that the variability amplitude should be larger than zero, 47, 39, 29, 24 and 18 objects are found to be radio-loud objects (with radio-loudness above 10) in g, r, i, z and y bands, respectively. We eliminate these objects. Ultimately, 8031, 8916, 9289, 8753 and 7325 objects are left to be radio-quiet NLS1 galaxies in g, r, i, z and y bands, respectively. The information on the time baseline and epoch number in g, r, i, z and y bands is displayed in Table 2.

3. Methods

By means of the variance of observed magnitudes, we obtain the variability amplitude which is the revised contribution from the measurement errors in the data sets (Sesar et al. 2007; Rakshit & Stalin 2017; Rakshit et al. 2019). The expression is as follows,

$$\Sigma = \sqrt{\frac{1}{N-1}\sum_{i=1}^{N}(m_i - \langle m\rangle)^2}, \quad (1)$$

where m_i is the ith magnitude and $\langle m\rangle$ is the average magnitude in the data sets. The error ϵ is expressed as

$$\epsilon^2 = \frac{1}{N}\sum_{i=i}^{N}\epsilon_i^2, \quad (2)$$

in which ϵ_i is the ith error. At last, the expression of the variability amplitude is

$$\sigma_m = \begin{cases}\sqrt{\Sigma^2 - \epsilon^2}, & \text{if } \Sigma > \epsilon,\\ 0, & \text{otherwise.}\end{cases} \quad (3)$$

Compared with other methods, it calculates the variability amplitude directly with the model-independent method, and also takes the impact of photometric errors into account.

Considering that the starlight contamination from the host galaxy of NLS1 galaxies is not negligible, we revise it by the method of Shen et al. (2011) which provided us an empirical fitting formula of the average host contamination, $\frac{L_{5100,\mathrm{host}}}{L_{5100,\mathrm{QSO}}} = 0.8052 - 1.5502x + 0.9121x^2 - 0.1577x^3$ for $x + 44 \equiv \log(L_{5100,\mathrm{total}}/\mathrm{erg\ s^{-1}}) < 45.053$. We extend it to $x < 0$ due to the low luminosity of NLS1 galaxies. No correction is needed for luminosities above this value. In the formula, the rest-frame luminosity at 5100 Å is from the catalog of the NLS1 sample. From the distribution of luminosity in 5100 Å, the fractional host contamination is depicted in the left and middle panel of Figure 1. The histogram distribution of variability amplitude in r band is displayed in the right panel of Figure 1. The green histogram is revised by the host galaxy contamination but the blue one is not revised. The median value of the variability

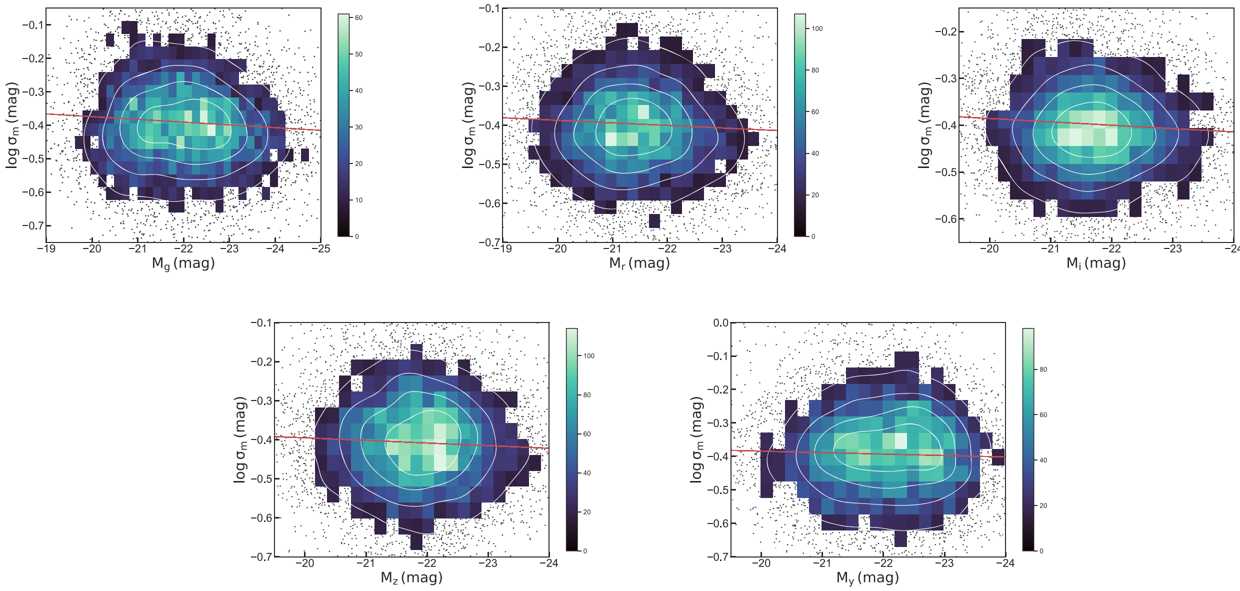

Figure 2. The relation between variability amplitude σ_m and absolute magnitude in g, r, i, z and y bands for the sample of NLS1 galaxies.

Table 3
The Relation Between Variability Amplitude σ_m and Luminosity in the NLS1 Galaxy Sample

	Spearman Correlation Coefficient	p value	Expression
$\sigma_{\rm m} - g$	0.064	6.184×10^{-20}	$-0.010x - 0.210$
$\sigma_{\rm m} - r$	0.042	4.969×10^{-5}	$-0.065x - 0.256$
$\sigma_{\rm m} - i$	0.055	4.294×10^{-10}	$-0.007x - 0.242$
$\sigma_{\rm m} - z$	0.040	2.051×10^{-4}	$-0.007x - 0.262$
$\sigma_{\rm m} - y$	0.022	2.069×10^{-4}	$-0.004x - 0.297$

amplitude is 0.149 mag, 0.124 mag, 0.113 mag, 0.123 mag and 0.178 mag in g, r, i, z and y band, respectively. After correcting the host contamination, the median variability amplitude is 0.397 mag, 0.392 mag, 0.391 mag, 0.390 mag and 0.408 mag, respectively.

4. Results and Discussions

4.1. The Relationship between Variability Amplitude and Absolute Magnitude in g, r, i, z and y Bands

In this section, we investigate the relationship between variability amplitude and absolute magnitude in g, r, i, z and y bands. The variability amplitude is calculated by expression (3). The absolute magnitude reflects the intrinsic luminosity of the source. Because of the intrinsic variation, we adopt the mean value of the absolute magnitude during the time span. The results are displayed in Figure 2 and Table 3. Our results show weak anti-correlations. An anti-correlated relationship between variability and luminosity was found in previous works adopting various AGN samples (Vanden Berk et al. 2004; Wilhite et al. 2008; Zuo et al. 2012). Most of them are focused on the quasar sample, and the variability work about NLS1 galaxy sample is sparse. The weak correlation in our results is consistent with the anti-correlation in the quasar sample, which indicates the mechanism of NLS1 galaxy in optical band may be similar with that of a quasar.

4.2. The Relation Between Variability Amplitude and Luminosity in 5100 Å, Black Hole Mass, Eddington Ratio, R_{4570} as Well as R_{5007}

In this section, we investigate the possible relationship between variability amplitude (g, r, i, z and y bands) and luminosity in 5100 Å (λL_{5100}), black hole mass $M_{\rm BH}$, Eddington ratio $\xi_{\rm Edd}$, R_{4570} and R_{5007}. By matching with the variability amplitude, 6299 objects are found with $\sigma_m > 0$. The analysis results in i band are listed in Figure 3. The Spearman coefficient, p value of no correlation and fitting expression are listed in Table 4.

4.2.1. The Relation Between Variability Amplitude and Luminosity in 5100 Å

We further investigate the relationship between variability amplitude and luminosity in 5100 Å. The variability amplitude σ_m is calculated by the method in Section 3. The luminosity is from Rakshit et al. (2017). The relation between variability amplitude and luminosity in 5100 Å is plotted in the upper left panel of Figure 3. The red line is the fitting result by the least squares method. A weak anti-correlation is apparent between

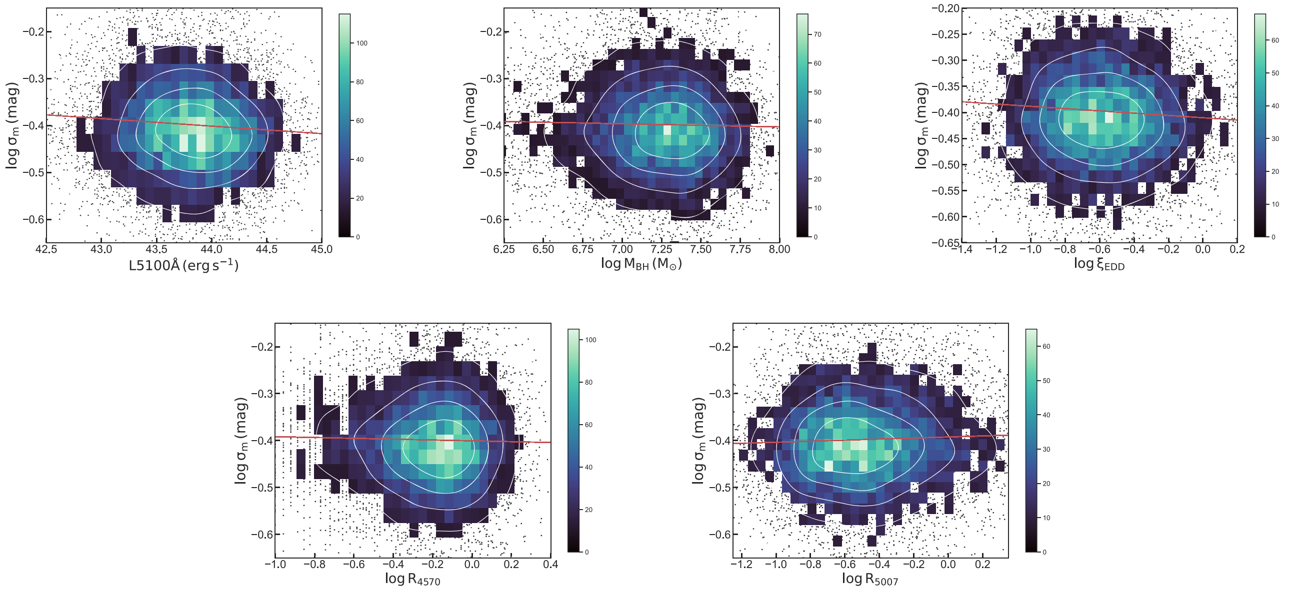

Figure 3. The relation between σ_m and luminosity in 5100 Å, black hole mass, Eddington ratio, R4570 as well as R5007 in the NLS1 galaxy sample.

Table 4
The Relation Between σ_m and Luminosity, Black Hole Mass, Eddington Ratio, R4570 as Well as R5007 in NLS1 Galaxy Sample

	Spearman Correlation Coefficient	p value	Expression
$\sigma_{\rm m}$ − L5100 Å	−0.060	3.981×10^{-20}	$-0.016x + 0.303$
$\sigma_{\rm m}$ − $\rm M_{BH}$	−0.065	2.906×10^{-10}	$-0.047x - 0.592$
$\sigma_{\rm m}$ − $\xi_{\rm Edd}$	−0.059	1.049×10^{-8}	$-0.051x - 0.960$
$\sigma_{\rm m}$ − logR4570	−0.023	3.613×10^{-23}	$-0.009x - 0.4005$
$\sigma_{\rm m}$ − logR5007	0.029	3.217×10^{-3}	$0.011x - 0.392$

variability amplitude and luminosity in 5100 Å, which is similar to the results in Section 4.1.

Ai et al. (2010) analyzed the multi-epoch photometric data sets of 58 NLS1 and 217 BLS1 AGNs from the Sloan Digital Sky Survey (SDSS) in the Stripe 82 region, and found the correlation between variability and luminosity is not significant. Rakshit & Stalin (2017) found the results presented anti-correlation in 11 101 NLS1 galaxies between variability amplitude and luminosity in 5100 Å for the CRTS with 5–9 yr data sets and a minimum of 50 epochs. Comparing with Ai et al. (2010) and Rakshit & Stalin (2017), we further verify the relation of anti-correlation from Pan-STARRS.

4.2.2. The Correlation Analysis Between Variability Amplitude and Black Hole Mass

We investigate the relationship between variability amplitude and black hole mass. The black hole mass is from Rakshit et al. (2017), in which they calculated them by the virtual motion of BLR clouds. A weak anti-correlation is apparent in the upper middle panel of Figure 3. Based on the data sets of 11 101 NLS1 galaxies from CRTS spanning 5–9 yr, Rakshit & Stalin (2017) found positive correlation in the $\sigma_d - M_{\rm BH}$ relation, which was also found in Ai et al. (2010), but Ai et al. (2010) further found the correlation disappeared when the dependency of $\lambda_{\rm Edd}$ was considered. Kelly et al. (2009) ascertained the amplitude of the short-timescale variations is significantly anti-correlated with black hole mass and luminosity with a sample of optical light curves for 100 quasars. They interpreted the optical flux fluctuations as resulting from thermal fluctuations that were driven by an underlying stochastic process, such as a turbulent magnetic field.

4.2.3. The Relationship between Variability Amplitude and Eddington Ratio

The Eddington ratio $\xi_{\rm Edd}$ is commonly considered to be the main driver of optical variability which is anti-correlated with the variability amplitude σ_m in optical band. The Eddington ratio is estimated by $\xi_{\rm Edd} = L_{\rm bol}/L_{\rm Edd}$, in which $L_{\rm bol} = 9 \times \lambda L_\lambda(5100\ \text{Å})$ erg s^{-1} and $L_{\rm Edd} = 1.3 \times 10^{38} M_{\rm BH}/M_\odot$ erg s^{-1} (Kaspi et al. 2000). The correlation between variability amplitude and Eddington ratio is presented in the upper right panel of Figure 3. The results display a weak anti-correlation which is similar with Ai et al. (2010) and Rakshit & Stalin (2017). Rakshit & Stalin (2017) analyzed the variability of a sample of 11 101 NLS1 galaxies and ascertained an anti-correlated relation between variability amplitude σ_m and Eddington ratio $\xi_{\rm Edd}$, which may be due to the uncertainties in the calculation of $M_{\rm BH}$ and L_{Edd}. Ai et al. (2010) found only

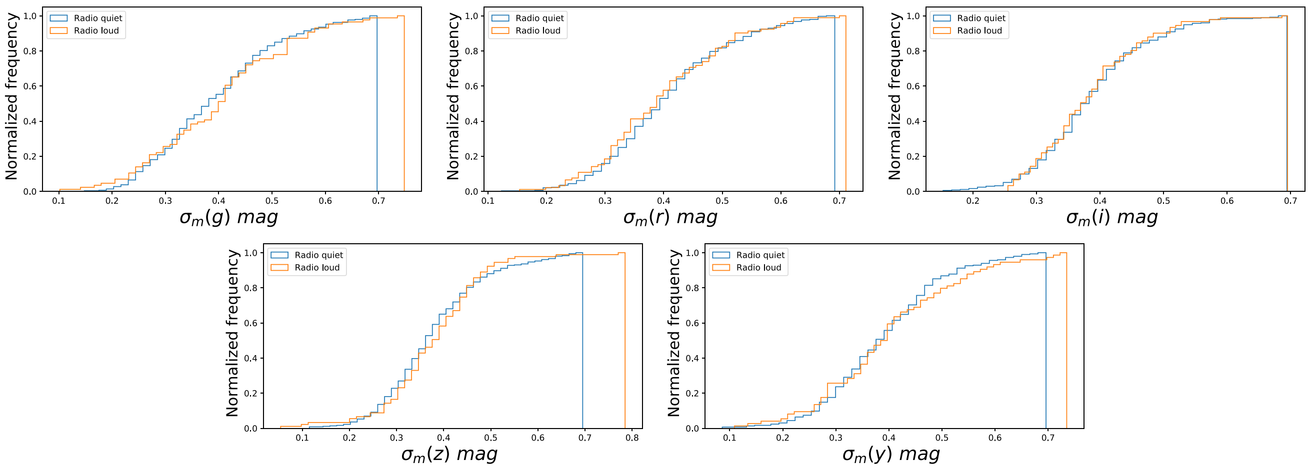

Figure 4. The cumulative σ_m and radio-loudness in NLS1 galaxies. The upper panel is the results in g band, r band and i band, from left to right respectively. The lower panel is the results in z band and y band, from left to right respectively.

marginal anti-correlation of the NLS1 sample by the multi-epoch data sets of SDSS. The anti-correlated relationship between optical variability and Eddington ratio has also been reported by many authors on the timescale of several months (Kelly et al. 2013) and several years (Wilhite et al. 2008; Bauer et al. 2009; MacLeod et al. 2010; Zuo et al. 2012; Meusinger & Weiss 2013) which can be understood from the simple standard accretion disk model (Shakura & Sunyaev 1973). If the emission originates from the inner accretion disk, the emission decreases as it propagates outward. As the Eddington ratio increases, the radius of the emission region at a given wavelength moves outward. The radius increases with the Eddington ratio since $r \sim T^{-1} \sim (\dot{m}/M_{\rm BH})^{1/3}\lambda^{4/3}$, where T is the temperature of the disk, λ is the wavelength and $\dot{m}$ is the mass accretion rate. Hence the variability amplitude σ_m decreases as the Eddington ratio increases.

4.2.4. The Correlation Analysis Between Variability Amplitude and R_{4570} as Well as R_{5007}

In this section, we investigate the relationship between variability amplitude and R_{4570} as well as R_{5007}. The Fe II strength R_{4570} is defined by the flux ratio of Fe II(λ4434-4684) to Hβ_b line, and R_{5007} is calculated by the flux ratio of the O[III] line to H$\beta_{\rm tot}$ line, which are taken from Rakshit et al. (2017). The O[III] line originates from the NLR, while Fe II and Hβ lines come from the broad line region. The variability amplitude is anti-correlated with R_{4570} in the lower left panel of Figure 3, but positively correlated with R_{4570} in the lower right panel of Figure 3, which is consistent with the results in Rakshit & Stalin (2017) and Rakshit & Stalin (2017) as R_{4570} is related to the Eddington ratio.

4.3. The Variability Characteristics of Radio Sub-sample

In order to understand the influence of radio emission on the observed optical flux variations, we construct a radio sub-sample of 555 objects by cross matching the NLS1 galaxy sample with the FIRST Survey. We get rid of the sources with zero variability. Ultimately, 331, 320, 306, 230 and 173 objects are left in g, r, i, z and y bands, respectively.

4.3.1. Comparison with the Amplitude of Radio Loud and Radio Quiet Samples

We perform a comparative analysis of the variability amplitude between radio-quiet and radio-loud NLS1 galaxies. The results of the cumulative distribution are depicted in Figure 4. The variability amplitude of the radio-loud sub-sample is slightly larger than that in the radio-quiet sub-sample in g band. No obvious difference was found between the variability amplitude of radio-loud and radio-quiet NLS1 galaxy samples in r, i, z and y bands.

4.3.2. The Relation Between Variability Amplitude and Radio Loudness

Rakshit & Stalin (2017) found the variability amplitude of radio-loud NLS1 galaxies in optical band is higher than that in radio-quiet NLS1 galaxies, which might be due to different physical processes in the two classes. They supposed that the optical emission in radio-loud objects originated from the presence of both non-thermal emission from the relativistic jet and thermal emission from the accretion disk. However, the optical emission was only due to the thermal emission from the accretion disk in radio-quiet objects.

The relation between variability amplitude and radio-loudness is depicted in Figure 5. It presents a weak positive

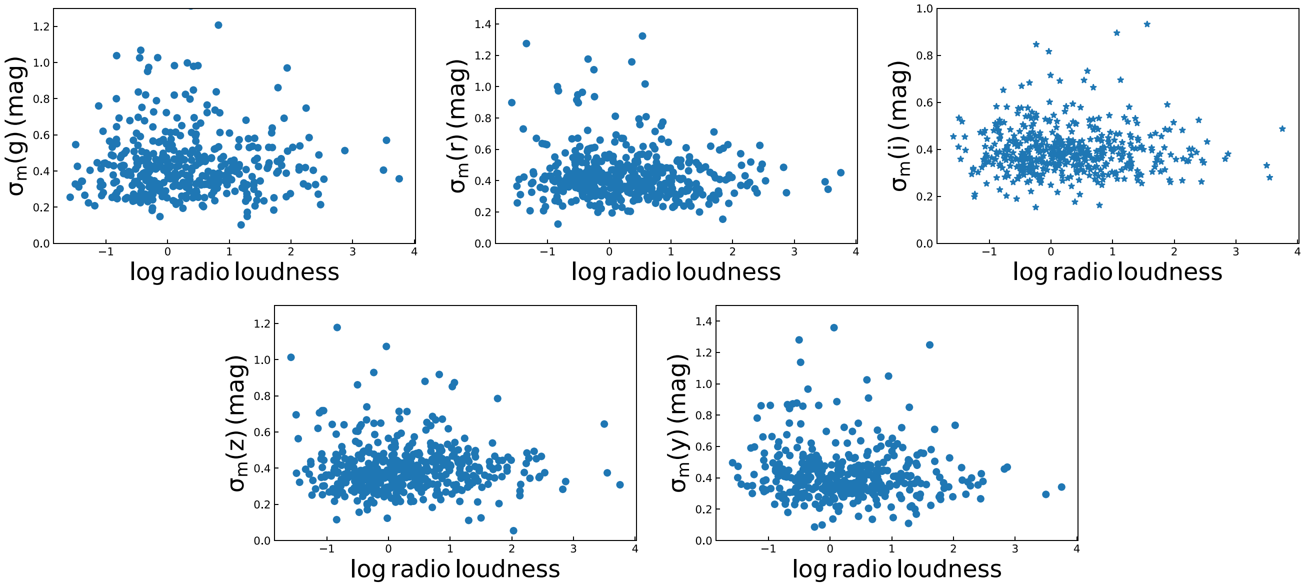

Figure 5. The relation between σ_m and radio-loudness in NLS1 galaxies. The upper panels are the results in g, r and i bands, from left to right respectively. The lower panels are the results in z and y bands, from left to right respectively.

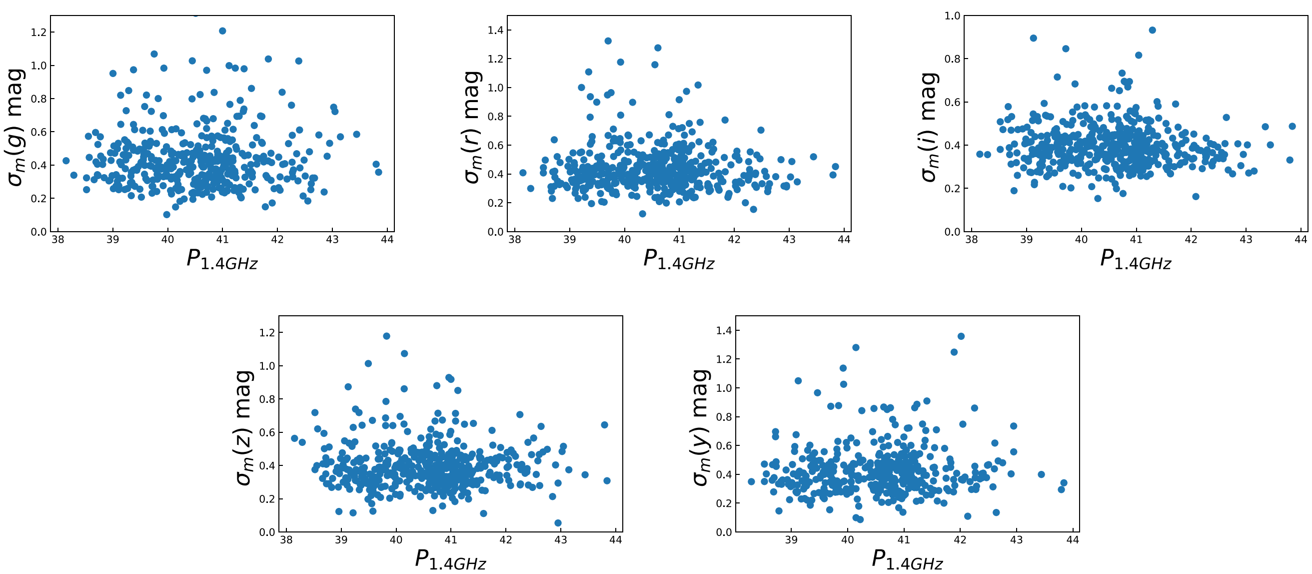

Figure 6. The relation between σ_m (g, r, i, z, y) and radio luminosity at 1.4 GHz in NLS1 galaxies. The upper panels are the results in g band, r band and i band, from left to right respectively. The lower panels are the results in z band and y band, from left to right respectively.

correlation in the upper panels (g and r bands) of Figure 5 which is consistent with the results in Rakshit & Stalin (2017). However, no obvious relation is visible in the other panels (i, z and y bands) of Figure 5.

In order to further verify the influence of radio emission on optical variability, we investigate the relationship between variability amplitude in g, r, i, z and y bands and luminosity at 1.4 GHz which has been revised by K-correction. The results are plotted in Figure 6. A weak positive correlation is visible in the upper left (g band) and middle (r band) panels of Figure 6, but no obvious results are in the other bands. We speculate that this may be due to the proximity in g and r bands to the fraction of continuum radiation in 5100 Å of the host galaxy contamination. The photometric values in i, z and y band are farther away from the 5100 Å band, which may lead to a larger correction error and thus the results become insignificant.

5. Conclusions

In this work, we systematically investigate the relationship between optical variability and many physical parameters for 11 101 NLS1 galaxies by data sets from the Pan-STARRS1 survey. The results are summarized as follows.

(1) We investigate the relationship between variability amplitude and absolute magnitude in g, r, i, z and y bands. The results show significant anti-correlations which are consistent with the results in previous works.
(2) The relationship between optical variability and many physical parameters (e.g., λL(5100 Å), black hole mass, Eddington ratio, R_{4570} and R_{5007}) is further analyzed. The results display significant anti-correlation with L(5100 Å), $M_{\rm BH}$, Eddington ratio and R_{4570}, but positive correlation with R_{5007}. This relation could be explained by the simple standard accretion disk model.
(3) The relationship between optical variability and radio luminosity/radio-loudness was analyzed. The results between optical variability and radio luminosity/radio-loudness manifest weak positive correlation in g and r bands, but insignificant correlation in i, z and y bands. The large error of the approximate fraction of host galaxies in i, z and y bands may induce insignificant correlations.

Acknowledgments

We thank Zhang Xueguang from Nanjing Normal University, Guo Xiaotong from Nanjing University and Lu Kaixing from Yunnan Observatories for the helpful comments and suggestions that improved this manuscript. This work is funded by the the Fundamental Research Funds for the Universities in Hebei Province (No: JYQ202003).

ORCID iDs

Xiao-Ling Yu https://orcid.org/0000-0002-2937-6699

References

Ai, Y. L., Yuan, W., Zhou, H., et al. 2013, AJ, 145, 90
Ai, Y. L., Yuan, W., Zhou, H. Y., et al. 2010, ApJL, 716, L31
Alam, S., Albareti, F. D., Allende Prieto, C., et al. 2015, ApJS, 219, 12
Bauer, A., Baltay, C., Coppi, P., et al. 2009, ApJ, 696, 1241
de Vries, W. H., Becker, R. H., White, R. L., & Loomis, C. 2005, AJ, 129, 615
Decarli, R., Dotti, M., Fontana, M., & Haardt, F. 2008, MNRAS, 386, L15
di Clemente, A., Giallongo, E., Natali, G., Trevese, D., & Vagnetti, F. 1996, ApJ, 463, 466
Doroshenko, V. T., Sergeev, S. G., Gaskell, C. M., et al. 2006, ARep, 50, 708
Gliozzi, M., Brinkmann, W., Räth, C., et al. 2002, A&A, 391, 875
Grupe, D., Thomas, H. C., & Beuermann, K. 2001, A&A, 367, 470
Guo, H., Wang, J., Cai, Z., & Sun, M. 2017, ApJ, 847, 132
Hawkins, M. R. S. 2000, A&AS, 143, 465
Helfand, D. J., Stone, R. P. S., Willman, B., et al. 2001, AJ, 121, 1872
Kaspi, S., Smith, P. S., Netzer, H., et al. 2000, ApJ, 533, 631
Kelly, B. C., Bechtold, J., & Siemiginowska, A. 2009, ApJ, 698, 895
Kelly, B. C., Treu, T., Malkan, M., Pancoast, A., & Woo, J.-H. 2013, ApJ, 779, 187
Klimek, E. S., Gaskell, C. M., & Hedrick, C. H. 2004, ApJ, 609, 69
Kshama, S. K., Paliya, V. S., & Stalin, C. S. 2017, MNRAS, 466, 2679
Lu, K.-X., Huang, Y.-K., Zhang, Z.-X., et al. 2019, ApJ, 877, 23
Ivezic, Ž., Lupton, R. H., Juric, M., et al. 2004, in The Interplay Among Black Holes, Stars and ISM in Galactic Nuclei, ed. T. Storchi-Bergmann, L. C. Ho, & H. R. Schmitt, Vol. 222 (Cambridge: Cambridge Univ. Press), 525
MacLeod, C. L., Ivezić, Ž., Kochanek, C. S., et al. 2010, ApJ, 721, 1014
Matthews, T. A., & Sandage, A. R. 1963, ApJ, 138, 30
Maune, J. D., Miller, H. R., & Eggen, J. R. 2013, ApJ, 762, 124
Meusinger, H., Hinze, A., & de Hoon, A. 2011, A&A, 525, A37
Meusinger, H., & Weiss, V. 2013, A&A, 560, A104
Osterbrock, D. E., & Pogge, R. W. 1985, ApJ, 297, 166
Paliya, V. S., Stalin, C. S., Kumar, B., et al. 2013, MNRAS, 428, 2450
Rakshit, S., Johnson, A., Stalin, C. S., Gandhi, P., & Hoenig, S. 2019, MNRAS, 483, 2362
Rakshit, S., & Stalin, C. S. 2017, ApJ, 842, 96
Rakshit, S., Stalin, C. S., Chand, H., & Zhang, X.-G. 2017, ApJS, 229, 39
Sesar, B., Ivezić, Ž., Lupton, R. H., et al. 2007, AJ, 134, 2236
Shakura, N. I., & Sunyaev, R. A. 1973, A&A, 500, 33
Shapovalova, A. I., Popović, L. Č., Burenkov, A. N., et al. 2012, ApJS, 202, 10
Shen, Y., Richards, G. T., Strauss, M. A., et al. 2011, ApJS, 194, 45
Ulrich, M.-H., Maraschi, L., & Urry, C. M. 1997, ARA&A, 35, 445
Vanden Berk, D. E., Wilhite, B. C., Kron, R. G., et al. 2004, ApJ, 601, 692
Welsh, B. Y., Wheatley, J. M., & Neil, J. D. 2011, A&A, 527, A15
Wilhite, B. C., Brunner, R. J., Grier, C. J., Schneider, D. P., & vanden Berk, D. E. 2008, MNRAS, 383, 1232
Xu, D., Komossa, S., Zhou, H., et al. 2012, AJ, 143, 83
Zuo, W., Wu, X.-B., Liu, Y.-Q., & Jiao, C.-L. 2012, ApJ, 758, 104